Tunable wavelength filters using polymer long-period waveguide gratings based on metal-cladding directly defined technique*

Ji-Hou Wang(王继厚), Chang-Ming Chen(陈长鸣)†, Yang Zheng(郑洋), Xi-Bin Wang(王希斌), Yun-Ji Yi(衣云骥), Xiao-Qiang Sun(孙小强), Fei Wang(王菲), and Da-Ming Zhang(张大明)

State Key Laboratory on Integrated Optoelectronics, College of Electronic Science and Engineering, Jilin University, Changchun 130012, *China*

(Received 28 June 2016; revised manuscript received 4 November 2016; published online 10 January 2017)

In this work, long-period waveguide grating-based tunable wavelength filters using organic–inorganic grafting poly(methyl methacrylate) (PMMA) materials are designed and fabricated by metal-cladding directly defined technique. The thermal stabilities and optical properties of the organic–inorganic grafting PMMA core materials are analyzed. Structures and performance parameters of the waveguide gratings and self-electrode heaters are designed and simulated. The contrast of the filter is about 15 dB and the resonant wavelength can be tuned by different electric powers applied to the metal-cladding self-electrode heaters. The temperature sensitivity is 3.5 nm/°C and the switching time is about 1 ms. The technique is very suitable for realizing the optoelectronic integrated wavelength-division-multiplexing systems.

Keywords: organic–inorganic grafting materials, polymer optical waveguide, long-period grating filter, metal-cladding defined technique

PACS: 42.79.Gn, 42.79.Dj, 72.80.Le **DOI:** 10.1088/1674-1056/26/2/024212

1. Introduction

Long-period waveguide gratings (LPWGs) are gratings in planar waveguide with grating period around 100 μm.[1–3] LPWGs-based devices have aroused considerable interest in recent years in the field of optical communication and sensor application because of the flexibility in waveguide structure and material as compared with the long-period fiber gratings.[4–8] Specially, LPWGs-based tunable wavelength filters are very suitable for realizing functional wavelength division multiplexing systems using optical planar integrated circuits. They can be compatible with other devices on silicon substrates, and can be produced in large quantities by using standard microelectronic processing techniques. Several material systems, including silicon-on-insulator (SOI), silicon, $LiNbO_3$ and polymers have been used to achieve LPWGs chip.[9–12] As a multi-functional material system, polymers exhibit well-controlled refractive indices, highly flexible structures, and large thermo–optic (TO) and electro–optic (EO) coefficients which can be conductive to realizing the monolithic integration with LPWGs-based tunable wavelength filter module.[13,14] At present, some studies have reported polymer LPWGs produced by reactive ion etching (RIE),[15] soft lithography,[16] or induced refractive index modulation.[17] In this paper, we propose a metal-cladding confinement waveguide structure to directly produce polymer LPWGs-based thermo–optic tunable wavelength filter based on organic–inorganic grafting PMMA materials. The thermal stabilities and optical properties of the hybrid materials are analyzed. Structural characteristics of the waveguide gratings and self-electrode heaters are provided. Optical performance parameters of the tunable wavelength filter are simulated and measured. The contrast and temperature sensitivity of the filter are obtained. The technique is advantageous in realizing the photonic multi-functional integrated circuits (PICs) WDM communication systems.

2. Experiment

2.1. Organic–inorganic grafting PMMA waveguide material

The organic–inorganic grafting PMMA waveguide material is synthesized by hydrolysis and polycondensation of 3-methacryloxy-proyltrimethoxysilane (MAPTMS, KH570), (3-glycidoxypropyl)trimethoxy-silane (GPTMS, KH560), methylmethacrylate (MMA), and tetrabutyl titanate ($Ti(OC_2H_5)_4$. The waveguide layer can form the grafting PMMA material with SiO_2–TiO_2 network. The molecular structure and synthesis process of the SiO_2–TiO_2 organic–inorganic grafting PMMA materials are given in Fig. 1. It shows the synthesis process of a PMMA network (a) and the structure of sol–gel core graft-modified material (b). The surface roughness value of the hybrid film scanned can be measured to be around 1.75 nm by atomic force microscope (AFM). Glass transition temperature (T_g) and thermal decomposition temperature (T_d) (5% loss) of the sol–gel material are measured to be 135 °C and 230 °C, respectively.

*Project supported by the National Natural Science Foundation of China (Grant Nos. 61575076, 61475061, and 61405070), the Fundamental Research Funds for the Central Universities, China (Grant No. JCKY-QKJC08), the Science and Technology Development Plan of Jilin Province, China (Grant Nos. 20130522151JH, 20140519006JH, and 20160520091JH), and the China Postdoctoral Science Foundation (Grant No. 2015M571362).

†Corresponding author. E-mail: chencm@jlu.edu.cn

© 2017 Chinese Physical Society and IOP Publishing Ltd

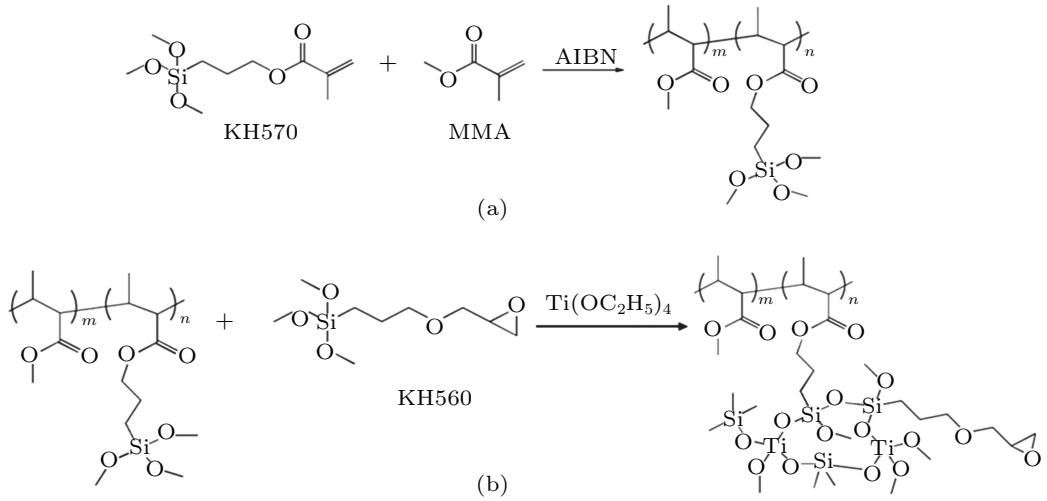


Fig. 1. Synthetic routes to (a) PMMA network and (b) sol–gel graft-modified material.

2.2. Tunable wavelength filter design and fabrication

The schematic diagram of a metal-cladding LPWG filter with self-electrode heaters is shown in Fig. 2(a). The thin gold grating structure is deposited directly on grafting PMMA waveguide layer. The metal-cladding grating of the filter can produce a significant index perturbation for power coupling between core and cladding modes. The metal grating is also designed and configured as self-electrode heater. When electric power is applied to the metal grating, the refractive index of the hybrid PMMA layer underneath the metal film is changed by thermo–optic effect. Effective wavelength tuning of the filter can be realized by changing the electric power to control the temperature of the self-electrode heater.

Figure 2(b) shows the cross-sectional structure of the metal-cladding defined waveguide gratings. Thermally oxidized silicon wafers are used as substrates, with oxide layer acting as the lower cladding. The grafting PMMA waveguide film is spinning-coated and cured onto silicon substrate. Double parallel Au strips are formed as metal upper claddings by the deposition and photolithography technique. The core waveguide structure is directly defined with air-upper cladding layer between the Au strips. The refractive indices of SiO_2, organic–inorganic grafting PMMA material, Au and air are 1.450, 1.508, $0.559 + 11.5i$, and 1.00 at 1550-nm wavelength, respectively. The mode distribution is calculated by software COMSOL multiphysics.

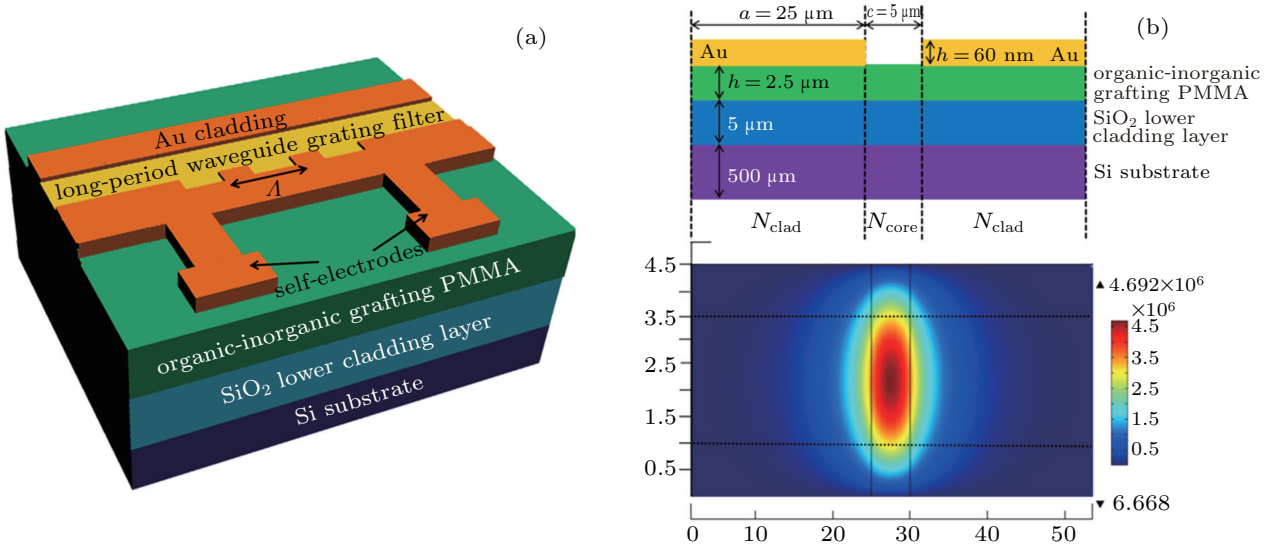


Fig. 2. (color online) (a) Schematic configuration of metal-cladding LPWG filter with self-electrode heaters; (b) cross-sectional structure of the metal-cladding defined waveguide and mode distribution calculated based on effective index method.

The relative eigenvalue equations based on effective index method[18] for the TM modes of core and cladding layers are defined, respectively. The effective index of core layer denoted as N_{core} is given as

$$k_0(n_1^2 - N_{core}^2)^{1/2} b = m\pi + 2\arctan\frac{n_1^2(N_{core}^2 - n_2^2)^{1/2}}{n_2^2(n_1^2 - N_{core}^2)^{1/2}}, \quad (m = 0, 1, 2, 3, \ldots). \tag{1}$$

The effective index of cladding layer denoted as N_{clad} is described as

$$k_0(n_1^2-N_1^2)^{1/2}b = n\pi+\arctan\frac{n_1^2(N_1^2-n_2^2)^{1/2}}{n_2^2(n_1^2-N_1^2)^{1/2}}+\arctan\frac{n_1^2(N_1^2-n_3^2)^{1/2}\delta_3}{n_3^2(n_1^2-N_1^2)^{1/2}},\quad (n=0,1,2,3,\ldots), \tag{2}$$

with

$$\delta_3=\frac{1+\dfrac{\varepsilon_3(N_1^2-n_4^2)^{1/2}-\varepsilon_4(N_1^2-n_3^2)^{1/2}}{\varepsilon_3(N_1^2-n_4^2)^{1/2}+\varepsilon_4(N_1^2-n_3^2)^{1/2}}\exp(-2k_0(N_1^2-n_3^2)^{1/2}h)}{1-\dfrac{\varepsilon_3(N_1^2-n_4^2)^{1/2}-\varepsilon_4(N_1^2-n_3^2)^{1/2}}{\varepsilon_3(N_1^2-n_4^2)^{1/2}+\varepsilon_4(N_1^2-n_3^2)^{1/2}}\exp(-2k_0(N_1^2-n_3^2)^{1/2}h)}, \tag{3}$$

$$k_0(n_1^2-N_2^2)^{1/2}b=n\pi+\arctan\frac{n_1^2(N_2^2-n_2^2)^{1/2}}{n_2^2(n_1^2-N_2^2)^{1/2}}+\arctan\frac{n_1^2(N_2^2-n_4^2)^{1/2}}{n_4^2(n_1^2-N_2^2)^{1/2}},\quad (n=0,1,2,3,\ldots), \tag{4}$$

$$k_0(N_1^2-N^2)^{1/2}a=m\pi+2\arctan\frac{N_1^2(N^2-N_2^2)^{1/2}}{N_2^2(N_1^2-N^2)^{1/2}},\quad (m=0,1,2,3,\ldots), \tag{5}$$

where n_1 is the refractive index of the core layer, n_2 is the refractive index of the bottom cladding, n_3 is the refractive index of the metal cladding, n_4 is the refractive index of the air, a is the width of the metal strips, h is the height of the metal strips, b is the thickness of the core waveguide, N_1 and N_2 are equivalent refractive indices of metal-both-side regions, respectively. It can be observed that the magnitude of the imaginary part of the effective refractive index is less than 10^{-5}, the value is so small that it can be ignored in the design of the waveguide device.

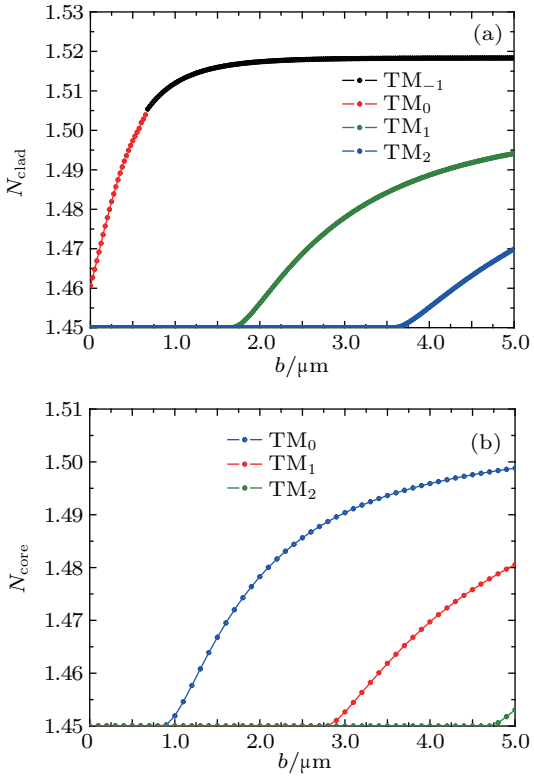


Fig. 3. (color online) Relations between the core thickness b and TM mode effective refractive indices of (a) the core and (b) the cladding for the resonant wavelength.

The relations between the core thickness b and TM mode effective refractive indices of the core and the cladding for the resonant wavelength are shown in Figs. 3(a) and 3(b), respectively. When the core thickness$b$is chosen to be 2.5 μm, there is only TM_0 mode in the core waveguide, and TM_0 mode in the cladding is cut-off. TM_{-1} mode in the cladding belongs to the surface plasmon polariton (SPP) mode in the Au cladding structure. The effective refractive index of TM_{-1} mode in the cladding is larger than that of TM_0 mode in the core waveguide, so there is no mode coupling between them.

As the LPWG filter, significant power coupling between TM_0 mode in the core waveguide and TM_m mode in the cladding is expected to occur at the resonance wavelength $\lambda_0=(N_{\rm core}-N_{\rm clad})\Lambda$, where Λ is the grating pitch. The LPWG filter is designed to operate at a grating pitch of 98 μm with an off-resonance wavelength of 1550 nm. The width of the core waveguide is 5 μm. The width and the height of the metal strips are defined as 25 μm and 60 nm, respectively. The corrugation depth is 2 μm, and the duty cycle is 50%. The grating length L is 5.0 mm. The transmission spectrum of the LPWG filter is given by[19]

$$T=1-\frac{k^2}{k^2+\delta^2/4}\sin^2\left(\sqrt{k^2+\frac{\delta^2}{4}}L\right), \tag{6}$$

where $\delta=(2\pi/\Lambda)(\lambda_0-\lambda)/\lambda$ is a detuning parameter (phase mismatch) that measures the deviation of the operation wavelength from λ to λ_0, L is the grating length, and κ is the coupling coefficient. For the TM polarization, the coupling coefficient κ, denoted as $\kappa_{\rm TM0\to TMm}$, is given by the spatial overlap between the two coupled modes over the grating area

$$k_{\rm TM0\to TMm}=k_x+k_z, \tag{7}$$

with

$$k_x=\frac{k_0(N_{\rm core}^2-N_{\rm clad}^2)N_{\rm core}N_{\rm cladm}}{2\pi c\varepsilon_0 N_{\rm core}^2N_{\rm clad}^2}\times\left(\frac{N_{\rm clad}^2}{N_{\rm core}^2}\int_{T_0}^{T_0+\Delta T}\int_{c-\Delta h}^{c-\Delta h/2}H_{0y}H_{my}U(x,t)\,{\rm d}x{\rm d}T+\frac{N_{\rm core}^2}{N_{\rm clad}^2}\int_{T_0}^{T_0+\Delta T}\int_{c-\Delta h/2}^{c}H_{0y}H_{my}U(x,t)\,{\rm d}x{\rm d}T\right),$$

$$k_z=\frac{(N_{\rm core}^2-N_{\rm clad}^2)}{2\pi c\varepsilon_0 k_0 N_{\rm core}^2N_{\rm clad}^2}$$

$$\times \int_{T_0}^{T_0+\Delta T} \int_{c-\Delta h}^{c} \frac{\partial H_{0y}}{\partial x} \frac{\partial H_{my}}{\partial x} U(x,t)\,\mathrm{d}x\mathrm{d}T,$$

where c is the speed of light in the vacuum, the ε_0 is the electric permeability of the vacuum, H_{0y} and H_{my} are the normalized magnetic fields for the TM_0 and TM_m modes, respectively. The coupling coefficient $\kappa_{TM0\to TMm}$ can be modulated by the TO effect through self-electrode heaters of the tunable LPWG filter.

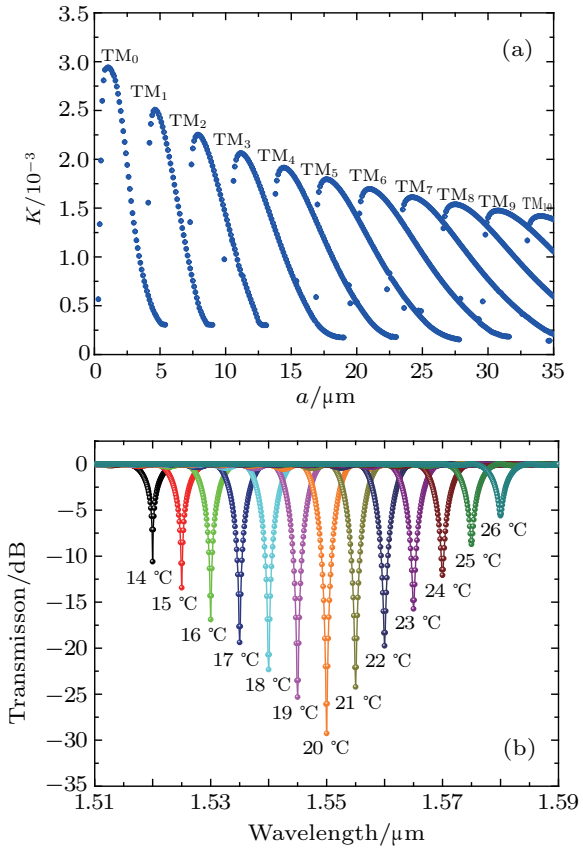


Fig. 4. (color online) (a) Dependence of the coupling coefficient on the cladding thickness for cladding TM modes and (b) transmission spectra of the LPWG filter for TM polarizations at different temperatures on the self-electrode.

The dependence of the coupling coefficient on the cladding thickness is shown in Fig. 4(a) for several cladding TM modes. It is seen from Fig. 4(a) that the coupling coefficient increases with cladding thickness increasing initially and reaches a maximum value at a particular cladding thickness. then decreases with cladding thickness further increasing. With $L = 5$ mm, the coupling coefficient required for achieving a maximum contrast is 3×10^{-4} μm^{-1} obtained from $\kappa = \pi/2L$. When electric power is applied to the self-electrode, heat is generated periodically along the filter, which generates a thermo–optic grating. The transmission spectra of the LPWG filter for TM polarizations at different temperatures on the self-electrode with the tunable resonant wavelength function are simulated as shown in Fig. 4(b). The resonant wavelength for TM polarization shifts toward the longer wavelength with the temperature increasing at a sensitivity of 5 nm/°C. The resonant wavelength can be tuned over the $C+L$-band with a temperature control of 12 °C. The maximum contrast of the rejection band is about 20 dB at room temperature for the resonant wavelength 1550 nm. The value of the contrast can also be modulated when the temperature of the self-electrode changes.

This LPWG filter is directly achieved by photolithography fabrication process forming Au-cladding defined structure. Figure 5(a) gives structural patterns of double gold claddings and long-period waveguide grating region by microscope (×500). It shows that the parameters designed of the metal-cladding directly defined waveguide grating can be realized well and the process enables the precise control of the core size. Figure 5(b) shows the surface morphology from the gold cladding measured by atomic force microscope (AFM). The thickness is about 60 nm and the surface roughness is less than 1.5 nm. The total resistance of the electrode is measured to be 2 kΩ.

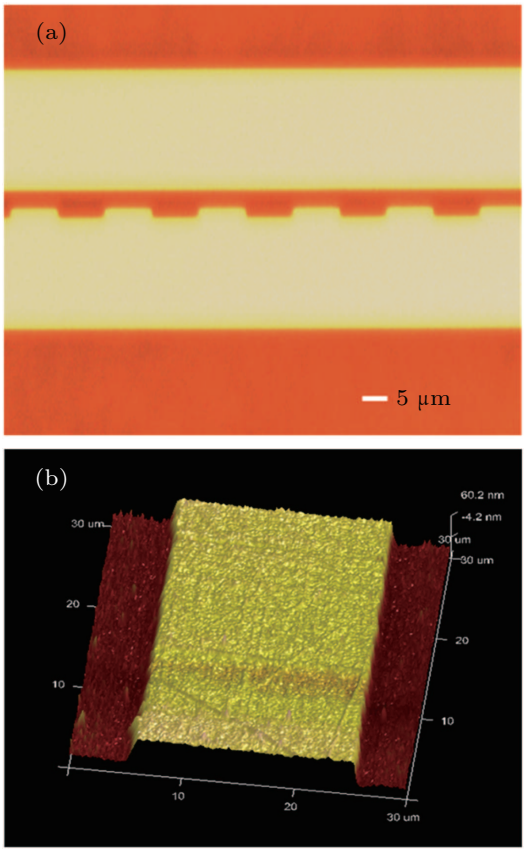


Fig. 5. (color online) (a) Structural patterns of double gold claddings and waveguide region by microscope (×500), and (b) surface morphology from the gold cladding measured by AFM.

2.3. Device measurement and discussion

The fabricated metal-cladding LPWG filters are characterized by launching light at wavelengths of 1510 nm–1590 nm from an amplified spontaneous emission (ASE)

source into the waveguide from a standard single-mode fiber, and by monitoring the output on an infrared camera, a photodetector and an optical spectrum analyzer. The transmission loss of the direct waveguide with 5-μm width is measured to be 1.2 dB/cm by a cut-back method. When electric power is applied to the self-electrode, heat is generated periodically along the waveguide, which generates a thermo–optic grating effect. Figure 6(a) shows the transmission spectra for the TM polarization measured for different electric powers applied to the electrode. As shown in Fig. 6(a), when the power is enhanced from 0 mW to 21 mW, the temperature of the electrode increases from 20 °C to 24 °C. The contrast of the rejection band decreases from 15 dB to 10 dB. The actual sensitivity of the filter is 3.5 nm/°C. Figure 6(b) shows the TO switching response observed by applying square-wave voltage at a frequency of 70 Hz. The switching rise and fall times are measured to be 1.1 ms and 1.2 ms, respectively. The actual electric power required for the LPWG filter to achieve maximum contrast change is about 30 mW. The lower power consumption and the faster response of the device are mainly dependent on the metal-cladding directly defined waveguide technique with self-electrode structure.

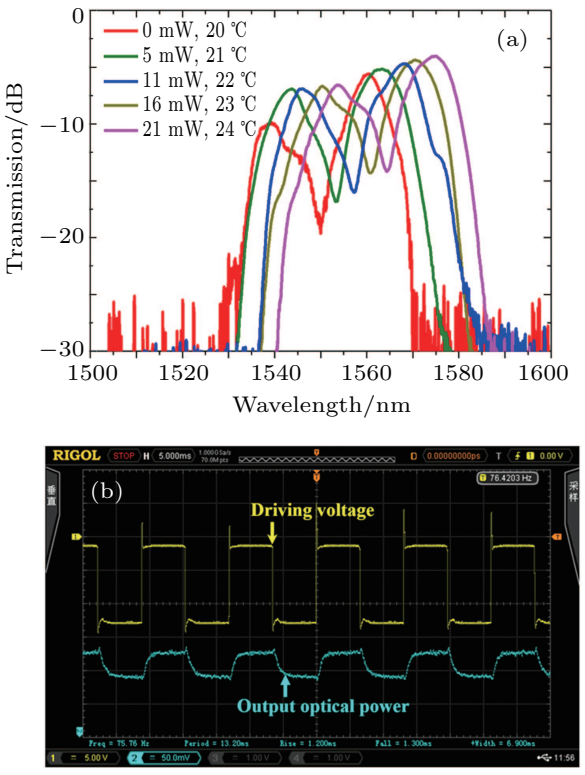


Fig. 6. (color online) (a) Transmission spectra measure actually for the TM polarization with different electric powers applied to the electrode and (b) TO switching response by applying square-wave voltage at a frequency of 70 Hz.

Compared with the ideal simulated parameters of the filters, the actually measured values of temperature sensitivity, contrast and insertion loss are slightly lower, which may be due to the fact that heat dissipation in actually measured process affects the thermal efficiency of metal self-electrodes and thus temperature sensitivity is disturbed. The contrast might be influenced by machining accuracy in the fabricating process for the ridge height of the gratings. By taking into consideration the absorption loss of the actual waveguide material and the coupling loss between the fiber and the waveguide, the actual insertion loss of the device measured is larger than the calculated value. However, in contrast to other results reported, there are still certain advantages in the key parameters of our device. For the reported TO tunable polymer LPWG filter devices,[20–22] including our device, the contrast is obtained mainly in a range of 10 dB–30 dB. The switching rise and fall times and the sensitivity are put into perspective by comparing with the performances of the other devices published in the literature as given in Table 1. It can be observed that the proposed TO tunable metal-cladding LPWG filter could achieve faster switching rise and fall times and higher sensitivity.

Table 1. Comparison of other published results for polymer LPWG filter device with our results.

Contrast/dB	(Switching rise/ fall times)/ms	Sensitivity/(nm/°C)	Reference
27	42/39	Less than 0.2	[20]
28	19/27	2	[21]
11	59/55	–	[22]
15	1.1/1.2	3.5	present work

3. Conclusions

In this study, we propose and demonstrate TO tunable LPWG filters based on organic–inorganic grafting PMMA materials by using the metal-cladding directly defined technique. The optical characteristics of the SiO_2–TiO_2 grafting PMMA material are analyzed. T_g and T_d of the hybrid material are measured to be 135 °C and 230 °C, respectively. Performance parameters of the device are designed and simulated. The contrast of the rejection band for the center wavelength is 15 dB, and 30 mW electric power applied to self-electrode heaters can achieve a maximum contrast change. The temperature sensitivity of the filter is about 3.5 nm/°C. The switching rise and fall times are measured to be 1.1 ms and 1.2 ms, respectively. The chip could improve the flexibility for the optoelectronic integrated circuits.

References

[1] Jiang J, Callender C L and Ledderhof C J 2010 *IEEE Photon. Technol. Lett.* **22** 951
[2] Zhou X J, Shi S H and Zhang Z Y 2012 *J. Photon.* **4** 119
[3] Garg R and Thyagarajan K 2013 *Appl. Opt.* **52** 2086
[4] Guo X W, Zhang X X and Li H P 2010 *Optoelectron.* **55** 1338
[5] Zhang Y W, Li Y F and He Z 2011 *Opt. Commun.* **284** 1828

[6] Kwon M 2010 *Opt. Lett.* **35** 3835
[7] Zhang D L, Kang J and Wong W H 2015 *Opt. Lett.* **40** 4715
[8] Semwal G and Rastogi V 2016 *Opt. Commun.* **359** 336
[9] Liu Q, Gu Z H and Kee J S 2014 *Opt. Lett.* **22** 29954
[10] Jin W and Chiang K S 2015 *Opt. Lett.* **40** 237
[11] Chuang R W, Hsu M T and Wang G S 2014 *Jpn. J. Appl. Phys.* **53** 04EG15 1–4
[12] Yang Y, Chen K X and Jin W 2015 *IEEE Photon. Technol. Lett.* **27** 1985
[13] Cai Y J, Li M, Yu L, *et al*. 2015 *Chin. Phys. Lett.* **32** 107305
[14] Yi J P, Chi L, Chen J S, *et al*. 2016 *Acta Phys. Sin.* **65** 056101 (in Chinese)
[15] Chu Y M, Chiang K S and Liu Q 2006 *Appl. Opt.* **45** 2755
[16] Jiang J, Callender C L and Jacob S 2012 *IEEE Photon. Technol. Lett.* **24** 2169
[17] Kwon M S and Shin S Y 2005 *IEEE Photon. Technol. Lett.* **17** 145
[18] Chen C M, Sun X Q, Wang F, Zhang F, Wang H, Shi Z, Cui Z C and Zhang D M 2012 *J. Quantum Electron.* **48** 61
[19] Rastogi V and Chiang K S 2002 *Appl. Opt.* **41** 6351
[20] Kwon M S and Shin S Y 2005 *J. Sel. Top. Quantum Electron.* **11** 190
[21] Chiang K S, Chow C K, Liu Q, Chan H P and Lor K P 2006 *IEEE Photon. Technol. Lett.* **18** 1109
[22] Lor K P, Chiang K S, Liu Q and Chan H P 2011 *IEEE Photon. Technol. Lett.* **23** 155